AIAA 79-0572R

Far-Field Condition in Jet Noise Experiments

U. Michel*
DFVLR, Abteilung Turbulenzforschung, Berlin (West), FRG
and
H. V. Fuchs†
Institut für Bauphysik, Stuttgart, FRG

The far-field condition is considered that has to be fulfilled when jet noise radiation data are compared. It becomes critical particularly when the jet flow is radiating as one coherent source extending over many jet diameters D in the axial and radial directions. To illustrate this, the jet is modeled by a distribution of 160 discrete, fixed point sources. The jet turbulence is simulated by a convected Gaussian turbulence. The deviation of the acoustical pressure field at a finite distance from the nozzle from the ideal far field at an infinite distance is studied numerically. The geometrical near-field effect is studied by assuming the point sources to be incoherent. It is strongest for small Strouhal numbers and far-field points near the jet axis. The interference effects which come into play if the sources are coherent are generally strongest for small Strouhal numbers in the direction of maximum jet noise radiation. Whereas the geometric near-field effect depends on Strouhal number, the interference near-field effect depends in addition strongly on the Mach number. For the error due to a finite source-observer distance to be less than 1 dB at the Strouhal number $St=0.1$, the measuring distance from the jet nozzle should be at least 120 jet diameters for an incoherent source and even longer for a coherent jet.

Introduction

DIFFERENTIATION between near and far fields is common practice when dealing with sound radiation problems of any kind. A clear definition is, however, difficult when the source with typical dimensions L_s is noncompact, meaning not small compared to the wavelength λ radiated. This is particularly true when the source radiates in a coherent manner. Yet comparatively little attention is devoted to this fundamental question in standard textbooks. Requiring the distance r to be at least one wavelength away from the closest source point for a representative far-field measurement may suffice in cases where one is interested in a noise datum of, e.g., a piece of machinery running under well-defined reference conditions. The far-field conditions become very essential, however, when scaling laws for the noise of a given source are to be derived which would enable a comparison of results obtained at, e.g., different power settings. This is exactly the aim of countless experimental jet noise studies (model and full-scale).

Jet noise directivity measurements of the sound pressure level (SPL) (R,θ) with the ambient fluid at rest are usually made with microphones placed on a circle with radial distance R from the center of the nozzle exit plane as a function of the polar angle θ to the jet axis. In the following we shall always express R in multiples of the nozzle diameter D.

The noise measurements by Lush[1] of an unheated subsonic jet were performed at $R=120$. Lush also studied the effect of R on his results by using different nozzles with one larger and two smaller diameters corresponding to $R=60$, 240, and 480 (see Fig. 2 of Ref. 1). He concluded that $R=120$ was sufficient to avoid unwanted near-field effects.

Ahuja[2] also measured the noise of unheated jets at subsonic Mach numbers. His measuring distances $R=25$, 30, and 47 were considerably closer to the nozzle than those of Lush. In spite of this, he ruled out any spurious near-field effects in the low-frequency regime by comparing the results at $R=25$ and 47 (see Figs. 21 and 22 of Ref. 2). This statement obviously contradicts that of Lush. The measurements with heated and unheated supersonic jets reported by Tanna et al.[3] and by Tanna[4,5] were made at an intermediate distance, $R=72$.

In his experimental study on the role of large-scale structures in the generation of jet noise Moore[6] used a measuring distance of $R=47$ and conceded that this distance would be "not really sufficient to obtain the true geometric far field of the source at low frequencies." To get into the geometric far field to an accuracy of 0.5 dB at a Strouhal number $St=f\cdot D/U=0.1$ where U is the jet exit velocity "measurements would have to be made at a radius of approximately 300 jet diameters, and to obtain the angular directivity correct to 2°, measurements must be made at least 450 diameters from the nozzle."

Arndt et al.[7] compared the effect of various jet noise suppressors with a plain jet at a distance of $R=37.5$. Although these measurements may have been affected by the near field at low frequencies, the comparisons made there should nevertheless be valid as the near-field effects of the different jets tested can be assumed to be more or less the same.

The acoustic far-field condition for a point source and the additional geometric and interference far-field conditions of spatially extended sources are discussed in Ref. 8. In the present paper we will study numerically the deviation of the acoustical pressure field from the ideal far field at an infinite distance. This will enable us to derive, in a quantitative manner, how the far field is affected by an insufficient source-observer distance.

Theoretical Model Describing Deviations from an Ideal Jet Noise Far Field

The asymptotic approach to an idealized far field can be studied by considering the ratio

$$\beta=\frac{R^2W_{pp}}{\lim\limits_{R\to\infty}(R^2W_{pp})}=\frac{R^2W_{pp}}{(R^2W_{pp})_\infty} \tag{1}$$

Presented as Paper 79-0572 at the AIAA 5th Aeroacoustics Conference, Seattle, Wash., March 10-12, 1979; submitted Nov. 1, 1979; revision received Aug. 11, 1980.

*Scientist. (The paper was prepared during tenure of a National Research Council Senior Research Associateship at NASA Langley Research Center.)

†Senior Scientist, Fraunhofer Gesellschaft.

where W_{pp} is the power spectral density of the pressure at a field point $P(R,\theta)$. Due to an insufficient distance R, β may be either larger or smaller than unity. On a logarithmic scale,

$$\Delta\mathrm{SPL} = 10\mathrm{dB}\cdot\log_{10}\beta \tag{2}$$

gives the difference in sound pressure level of a measurement of $R^2 W_{pp}$ at the distance R as compared to a measurement at $R\to\infty$. ΔSPL will hereafter be termed "far-field error" for brevity. Measuring conditions where one can vary R ad libitum are very rarely found in real life. This may be the reason why no systematic investigation has become known which would have quantified the error due to only partial fulfillment of the far-field condition. This situation prompted us to calculate β numerically as a function of R. We assume the acoustic far-field condition to be fulfilled (pressure in phase with velocity fluctuations). W_{pp} can then be derived from Lighthill's equation. For a jet with constant mean density the solution for the pressure p in the point P with coordinates x_i of the acoustical far field is

$$p(x_i,t) = \frac{Ma^2}{4\pi R}\int_V \frac{R}{R_0}\frac{\partial^2 Q(y_i,t_r)}{\partial t^2}\,\mathrm{d}V \tag{3}$$

where R = distance of field point P from the nozzle, R_0 = distance of P from source point S (see Fig. 1), $Ma = U/a_0$ Mach number, where U = jet exit velocity and a_0 = speed of sound in the ambient fluid, y_i = coordinates of source point S, $t_r = t - R_0/a_0$ retarded time, $Q = \rho c_r^2 + p - \rho a_0^2$, where c_r is the component of the fluctuating velocity in the direction toward the field point P considered, p and ρ denote pressure and density in the source point S. All quantities are made dimensionless with nozzle diameter D, U, and density ρ_0 outside the jet.

The nondimensional autocorrelation function R_{pp} in the field point P is then

$$R^2 R_{pp}(x_i,\tau) = \frac{Ma^4}{(4\pi)^2}\int_V\int_V \frac{R^2}{R_{01}R_{02}}\frac{\partial^4}{\partial\tau^4} \times R_{Q_1Q_2}(\hat{\tau}+\tau)\,\mathrm{d}V_2\,\mathrm{d}V_1 \tag{4}$$

where R_{01}, R_{02} are distances of P from source points S_1 and S_2 (Fig. 1), $R_{Q_1Q_2}$ is the cross-correlation function of the source quantity Q at points S_1 and S_2, and $\hat{\tau} = (R_{02} - R_{01})/a_0$ is the difference of the retarded times at points S_2 and S_1.

One may note that R_{pp} is proportional to Ma^8, the well-known Lighthill power law for jets with constant mean density, if we normalize with the ambient speed of sound rather than the jet exit velocity. By Fourier transforming Eq. (4) we obtain the power-spectral density in the field point P.

$$R^2 W_{pp} = \pi^2 He^4 \int_V\int_V \frac{R^2}{R_{01}R_{02}} W_{Q_1Q_2} \times \exp[-2\pi i He(R_{02}-R_{01})]\,\mathrm{d}V_2\,\mathrm{d}V_1 \tag{5}$$

where $W_{Q_1Q_2}$ is the cross-spectral density of Q at the source points S_1 and S_2.

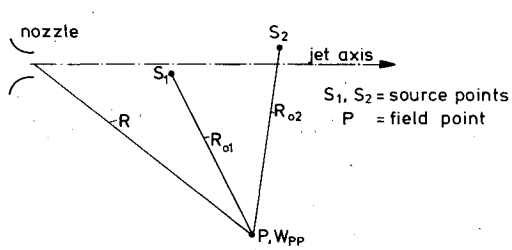

Fig. 1 Source points S_1 and S_2, field point P.

Equation (5) reveals that the Helmholtz number $He = Ma\cdot St$ where $St = f\cdot D/U$, is an important parameter for coherently radiating sources whenever $W_{Q_1Q_2} \neq 0$ for $S_1 \neq S_2$. Since the value of Q, and therefore also of $W_{Q_1Q_2}$, is a strong function of St and a weak function of Ma these two parameters also have an influence on $R^2 W_{pp}$. For our numerical study the double integral in Eq. (5) over the source volume is replaced by a twofold series,

$$R^2 W_{pp} = \pi^2 He^4 \sum_{k=1}^{K}\sum_{j=1}^{K} \frac{R^2}{R_j R_k} W_{jk}\exp[-2\pi i He(R_k - R_j)] \tag{6}$$

This is an equally exact representation if

$$W_{jk}(R,\theta) = \int_{\Delta V_j}\int_{\Delta V_k} \frac{R_j R_k}{R_{01}R_{02}} W_{Q_1Q_2}(R,\theta) \times \frac{\exp[-2\pi i\, He(R_{02}-R_{01})]}{\exp[-2\pi i\, He(R_k - R_j)]}\,\mathrm{d}V_2\,\mathrm{d}V_1 \tag{7}$$

The total source volume has simply been subdivided into K volume elements ΔV_j. R_j and R_k may be the distances of the centers of ΔV_j and ΔV_k from the observer point P. For sufficiently small ΔV_j Eq. (7) may be approximated by

$$W_{jk}(R,\theta) = W_{Q_jQ_k}(R,\theta)\cdot\Delta V_j \Delta V_k \tag{8}$$

For $R\to\infty$ we obtain from Eq. (6)

$$(R^2 W_{pp})_\infty = \pi^2 He^4 \sum_{j=1}^{K}\sum_{k=1}^{K} W_{jk}\exp[-2\pi i\, He(R_k - R_j)_\infty] \tag{9}$$

and hence, according to Eq. (1)

$$\beta(R,\theta) = \frac{\sum_{j=1}^{K}\sum_{k=1}^{K} W_{jk}\frac{R^2}{R_j R_k}\exp[-2\pi i\, He(R_k - R_j)]}{\sum_{j=1}^{K}\sum_{k=1}^{K} W_{jk\infty}\cdot\exp[-2\pi i\, He(R_k - R_j)_\infty]} \tag{10}$$

$W_{jk} = W_{jk}(R,\theta)$ and $W_{jk\infty} = W_{jk\infty}(\theta)$ may be replaced by the equations

$$W_{jk}(R,\theta) = Q_j(R,\theta)\cdot Q_k(R,\theta)\cdot W_{jk}^*(R,\theta) \tag{11}$$

and

$$W_{jk\infty}(\theta) = Q_{j\infty}(\theta)\cdot Q_{k\infty}(\theta)\cdot W_{jk\infty}^*(\theta) \tag{12}$$

$Q_j, Q_k, Q_{j\infty}$, and $Q_{k\infty}$ denote the strength of the sources at the respective source points and W_{jk}^* and $W_{jk\infty}^*$ the normalized cross-spectral densities. The values for $R\to\infty$ are only a function of the angle θ at which the nozzle is seen from the field point. For finite R the value of Q_j may change with R as the actual angle θ_j of the source point changes. The same is true for W_{jk}^*.

Until now the analysis is exact. Let us now assume the integral of Eq. (7) over small volume elements to be independent of R. This requires the following:

1) The differences between Q_j and $Q_{j\infty}$ be small. This would be strictly valid for point monopoles. Otherwise it would require the directivity of the sources to vary but slightly with angle θ_j or the difference between angles θ and θ_j to be small.

2) The differences between W_{jk}^* and $W_{jk\infty}^*$ be small. This requires the angular differences $\theta - \theta_j$ and $\theta - \theta_k$ to be of minor influence on W_{jk}^*.

With these two assumptions we get

$$W_{jk}(R,\theta) \cong W_{jk\infty}(\theta) = W_{jk}(\theta) = Q_j Q_k W_{jk}^* \tag{13}$$

and β becomes

$$\beta(R,\theta) = \frac{\sum_{j=1}^{K}\sum_{k=1}^{K} Q_j Q_k W_{jk}^*(\theta)\cdot\frac{R^2}{R_j R_k}\exp[-2\pi i\, He(R_k - R_j)]}{\sum_{j=1}^{K}\sum_{k=1}^{K} Q_j Q_k W_{jk}^*(\theta)\exp[-2\pi i\, He(R_k - R_j)_\infty]} \tag{14}$$

Since the $Q_j Q_k W_{jk}^*$ appear in both the numerator and denominator it is the variation of Q_j across the source volume V rather than its absolute strength that affects β.

The wave path R_k may be expressed in terms of R,θ,x_k,r_k, and ϕ_k (see Fig. 2).

$$R_k^2 = R^2\left(1 - \frac{x_k}{R}\cos\theta - \frac{r_k}{R}\sin\theta\cos\phi_k\right)^2 + x_k^2\sin^2\theta$$

$$+ r_k^2(1 - \sin^2\theta\cos^2\phi_k) - 2x_k r_k\sin\theta\cos\theta\cos\phi_k \tag{15}$$

For $R\to\infty$ and $r_j = r_k = r$ one obtains

$$(R_k - R_j)_\infty = (x_j - x_k)\cos\theta + r(\cos\theta_j - \cos\theta_k)\sin\theta \tag{16}$$

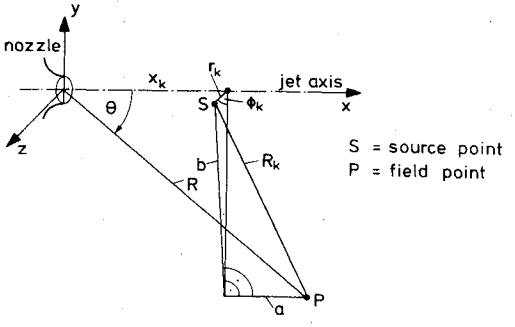

Fig. 2 Wave path length between source point S and field point P.

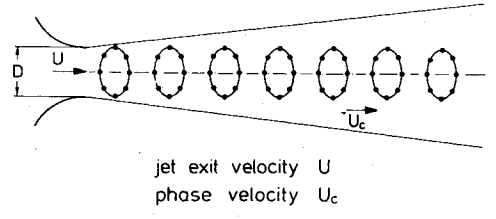

Fig. 3 Source locations of source model with $N=8$ and $M=7$ as example.

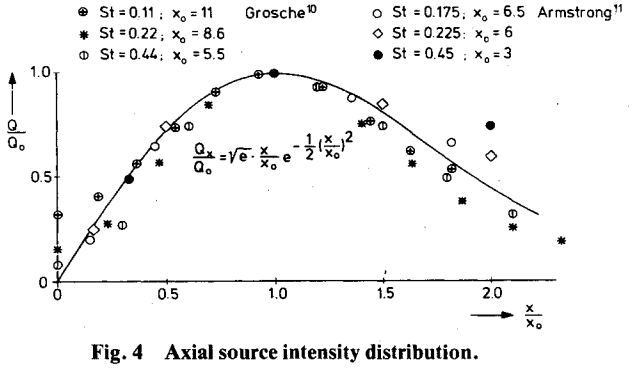

Fig. 4 Axial source intensity distribution.

For studying the transition from the near to the far field a limited number of $K=160$ source elements is chosen leading to K^2 discrete values of W_{jk}.

Our source models are then characterized as follows:

1) The sources are located on a circular cylinder (Fig. 3) at $N=4$ equidistant azimuthal and $M=40$ equidistant axial locations. In a recent paper Maestrello[9] used a similar model with $N=8$, $M=2$.

2) The strength of these sources is chosen as

$$Q(x,\theta) = Q_0(\theta)\frac{x}{x_0}\exp\left(-\frac{1}{2}\left(\frac{x}{x_0}\right)^2\right) \tag{17}$$

where

$$x_0 = x_0(St) \tag{18}$$

The location x_0 of the peak intensity $Q_0(\theta)$ is a function of St with, e.g., $x_0=12$ for $St=0.1$ and $x_0=7$ for $St=0.4$. This distribution is compatible with Grosche's[10] acoustical mirror measurements at 90 deg to the jet axis (Fig. 4). Fluctuating aerodynamic pressure intensity distributions as measured by Armstrong[11] with microphone probes inserted into the jet mixing zone display a similar behavior.

As already noted, the absolute strength $Q_0(\theta)$ does not affect β. All sources are assumed to have the same directivity $Q_0(\theta)$. This, likewise, has no effect on β as long as condition 1 is valid. The relative source strength distribution Q/Q_0 is considered to be uniform for all directions θ.

3) The spatial coherence of the sources is assumed to exhibit the same characteristic properties as determined from the pressure cross-spectral density measurements of Armstrong.[11] The normalized cross-spectral density at two source locations can then be described as

$$W_{jk}^* = C_\phi(\phi_k - \phi_j)\;C_x(x_k - x_j) \tag{19}$$

C_ϕ is a function of the azimuthal displacement $\Delta\phi$ of the point sources. It is regarded as the sum of a limited number μ of azimuthal constituents according to the source expansion scheme fully discussed in Ref. 12 [see Eq. (14) there].

$$C_\phi(\phi_k - \phi_j) = \sum_{m=0}^{\mu} A_m\cos[m(\phi_k - \phi_j)] \tag{20}$$

Similarly as in Ref. 13, for C_x we choose a "convected Gaussian" form,

$$C_x(x_k - x_j) = \exp\left[-\pi\left(\frac{x_k - x_j}{L_c}\right)^2\right]\cdot\exp\left[2\pi i\frac{St\,x_0}{U_c}\frac{(x_k - x_i)}{x_0}\right] \tag{21}$$

with the nondimensional axial displacement $(x_k - x_j)$ of the sources, a coherence length scale L_c, and the nondimensional phase velocity U_c.

Measurements of L_c are scarce. Armstrong[11] has measured the coherence of pressure signals at $x_j=3$, $r_j=0.5$ and at

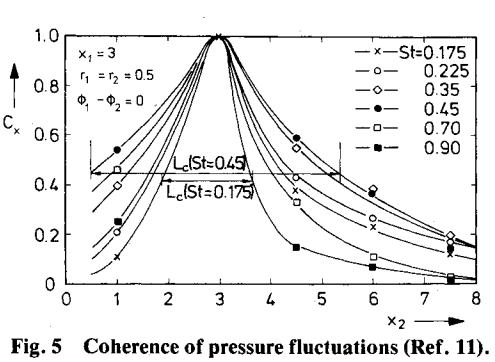

Fig. 5 Coherence of pressure fluctuations (Ref. 11).

varying $x_k, r_k, \phi_{jk} = 0$. Figure 5 is derived from his data for various Strouhal numbers and $r_k = 0.5$. The coherence length scale

$$L_c = \int_{-\infty}^{\infty} C_x(\Delta x)\,\mathrm{d}(\Delta x) \tag{22}$$

is largest for $St = 0.45$ which in his measurements was about the peak Strouhal number of the pressure power spectral density at $x_j = 3$ and $r_j = 0.5$.

Uncorrelated Source Model of Jet Noise

Before studying the influence of a coherent motion of the jet, the results for a small eddy model with no correlation between different sources are first derived for comparison. This specified model is characterized by

$$W_{jk} = \begin{cases} Q_j^2 & \text{for } j=k \\ 0 & \text{for } j \neq k \end{cases} \tag{23}$$

Equation (21) then reduces to,

$$\beta(R,\theta) = \sum_{j=1}^{K} Q_j^2 \frac{R^2}{R_j^2} \Big/ \sum_{j=1}^{K} Q_j^2 \tag{24}$$

Since R/R_j and Q_j depend on x_0 and x_0 in turn is a function of St, β can be written as

$$\beta = \beta(R,\theta,St) \tag{25}$$

Coherent Source Model of Jet Noise

For lack of a better knowledge of the variation of L_c in Eq. (21) with St and x the relative axial coherence length scale L_c/x_0 is kept constant across the total source region. The dimensionless phase velocity is assumed $U_c = 0.6$ in this analysis. The azimuthal coherence function C_ϕ was chosen as

$$C_\phi(0\text{ deg}) = 1,\ C_\phi(90\text{ deg}) = 0.4,\ C_\phi(180\text{ deg}) = 0.2 \tag{26}$$

As compared to the uncorrelated source, β depends additionally on the parameters Ma and L_c/x_0, if the sources are correlated. Thus, β is a function of the parameters

$$\beta = \beta(R,\theta,St,Ma,L_c/x_0) \tag{27}$$

Results

Uncorrelated Source Model

This model allows the effect of the noncompactness of the source region to be studied. Some results are depicted in Figs. 6 and 7 for the Strouhal number $St = 0.4$ and 0.1. In both cases the error is largest near the jet axis in the downstream and upstream quadrants. For $St = 0.4$ the error for $\theta = 15$ deg is less than 1 dB for a dimensionless distance $R_1 = 62$ from the nozzle. To reduce the error to 0.5 dB one has to double the distance to $R_{0.5} = 120$. The errors are much larger for the lower Strouhal number $St = 0.1$ since in this case the maximum source intensity is located further downstream at $x_0 = 12$. For a 1 dB error the necessary distance is $R_1 = 125$. At the distance $R = 50$ where many far-field measurements are made, the error is 2.8 dB at $\theta = 15$ deg, -0.4 dB at $\theta = 90$ deg, and -1.6 dB at $\theta = 135$ deg. It is noted that these results are obtained with $N = 4$ azimuthally displaced and $M = 40$ axially displaced source locations. Systematic examinations have shown, however, that the results change by less than 0.1 dB if $N = 2$ and $M = 20$ is used instead.

The results of the uncorrelated source model are a function only of x_0, the axial location of the peak source intensity. This in turn has been assumed to be a function of the Strouhal number St only. The Mach or Helmholtz number have no influence as was previously indicated by Eq. (25).

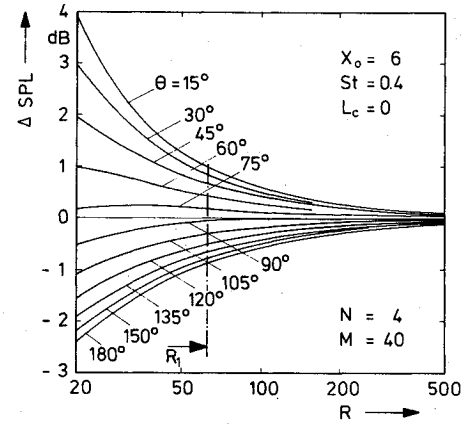

Fig. 6 Far-field error of uncorrelated source model as function of distance R from mode.

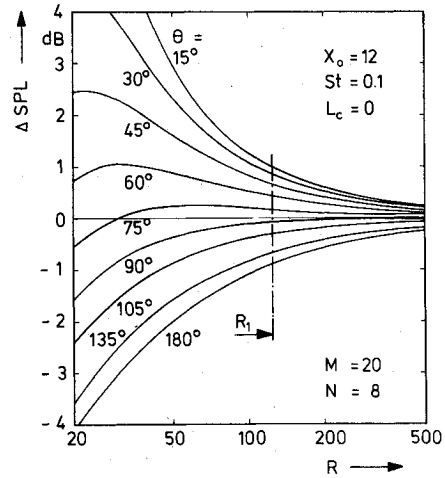

Fig. 7 Far-field error of uncorrelated source model as function of distance R from mode.

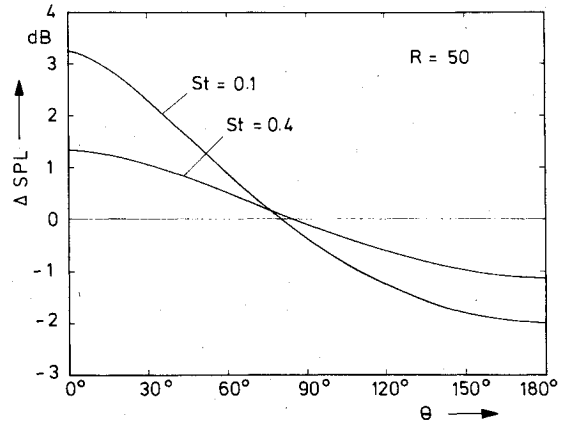

Fig. 8 Far-field error of uncorrelated source model as function of angle θ to jet axis.

For large values of x_0 the nozzle diameter should loose much of its influence, and β should be a function of R/x_0 and θ only. From the results for $St = 0.1$ and 0.4 the 1 dB error point is determined approximately by

$$R_1/x_0 = 10;\quad \theta = 15\text{ deg},\ \Delta\text{SPL} = 1\text{ dB} \tag{28}$$

This equation should also be valid for larger x_0, i.e., for smaller Strouhal numbers.

The results are replotted in Fig. 8 for $R = 50$ as a function of angle θ to the jet axis. The geometric near-field errors are

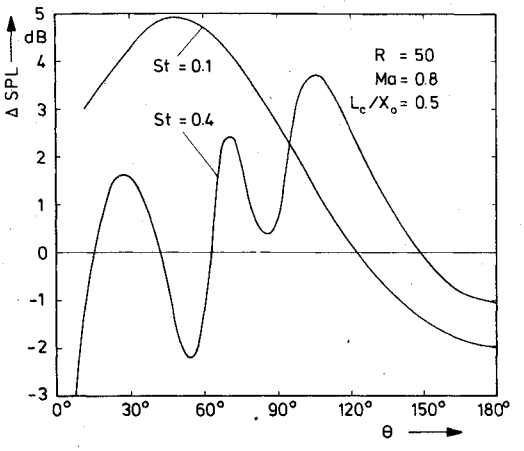

Fig. 9 Far-field error of coherent source model as function of angle θ to jet axis.

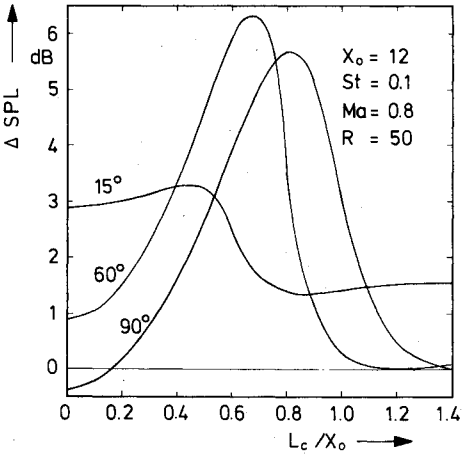

Fig. 11 Influence of coherence length scale L_c/x_0 on far-field error.

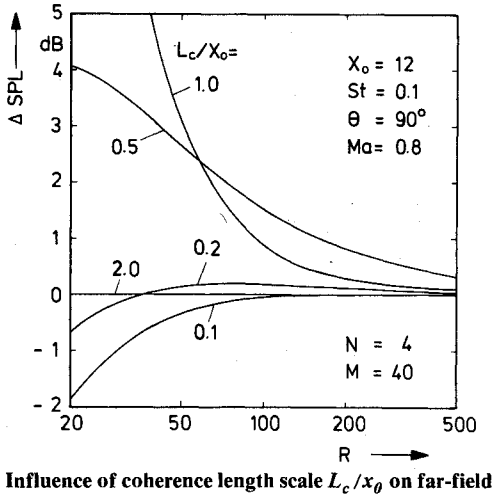

Fig. 10 Influence of coherence length scale L_c/x_0 on far-field error.

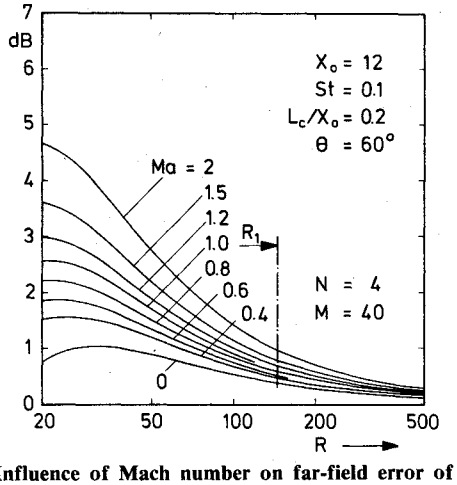

Fig. 12 Influence of Mach number on far-field error of coherent source model.

nearly antisymmetric for $\theta<90$ deg and $\theta>90$ deg. Due to the location of x_0 being downstream of the nozzle the errors are positive in the $\theta<90$ deg quadrant and negative for $\theta>90$ deg. The errors will therefore be much smaller if they are calculated relative to the point of peak intensity at $x=x_0$ rather than the nozzle exit.

Coherent Source Model

Influence of Strouhal Number

The introduction of an azimuthal and axial coherence of sources gives rise to additional interference effects in the far field which may decrease or increase the error due to a finite distance R. A result for $Ma=0.8$ and the relative coherence length scale $L_c/x_0=0.5$ is shown for $St=0.4$ and 0.1 in Fig. 9 for $R=50$ as a function of θ. The typical interference patterns become particularly clear at the higher Strouhal number. As compared to Fig. 8 the peak errors are generally larger. Figure 9 was obtained with arbitrarily chosen values of L_c/x_0 and Ma. In the following sections we will study the effect of these parameters.

Influence of Axial Coherence Length Scale L_c

In what follows we shall restrict ourselves to $St=0.1$. To demonstrate the effect of the coherence length scale the far-field error ΔSPL is plotted in Fig. 10 for $St=0.1$ and $\theta=90$ deg with L_c/x_0 as parameter.

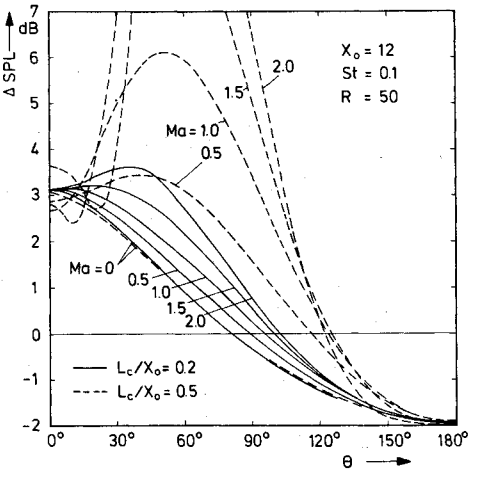

Fig. 13 Influence of Mach number on far-field error for two coherence length scales.

The error reaches a maximum value for L_c/x_0 between 0.5 and 1.0, as can be seen in Fig. 11. Increasing the coherence length scale beyond this critical range would result in a reduced far-field error.

In Fig. 9 we have taken $L_c/x_0=0.5$ which is approximately in accordance with Armstrong's turbulent pressure

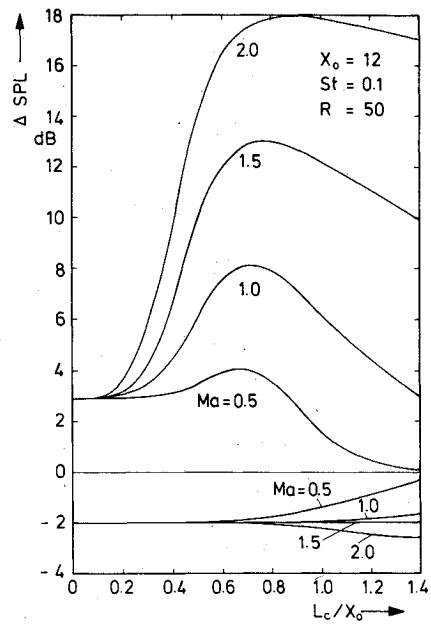

Fig. 14 Maximum far-field errors in whatever direction.

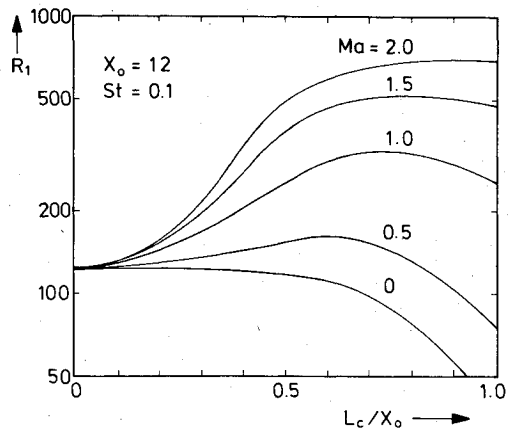

Fig. 15 Far-field distance R_1 from nozzle required to keep far-field error down to 1 dB.

measurements. This is now seen to represent about the most critical case with respect to the far-field error due to a finite R. We can see from Figs. 10 and 11 that the error due to interference effects is greatly reduced if a value of 0.2 is chosen for L_c/x_0. The results were found to be nearly insensitive to differing models describing the coherence between azimuthally displaced sources. This is a consequence of the Helmholtz numbers $He=D/\lambda=Ma\cdot St$ being small in the cases where large far-field errors are to be expected. The presented results were all obtained with the model according to Eq. (26) with $N=4$.

Influence of Mach Number

The Mach number becomes an important parameter for any coherent source model. In Fig. 12 one can see this influence of the Mach number on the error ΔSPL at $St=0.1$, $\theta=60$ deg for $L_c/x_0=0.2$. With increasing Mach number the error is steadily increased.

In Fig. 13 the error is plotted for $R=50$ as a function of the angle θ for the two length scales $L_c/x_0=0.2$ and 0.5. It can be seen how the error is increased nearer to the maximum jet noise radiation if L_c/x_0 or Ma is increased.

Conclusions

Two kinds of uncertainties may occur in jet noise experiments at necessarily limited far-field distances R. The first stems from the source having a finite extent L_s. The resulting error due to R not having reached the geometric far field is largest for θ approaching 0 or 180 deg and relatively small at $\theta=90$ deg. The second uncertainty arises when the whole, acoustically noncompact source region radiates in a coherent manner. The resulting wave interference may either increase or decrease the far-field error. Figure 14 presents the maximum positive and negative errors in whatever direction for different Mach numbers and $St=0.1$. The measuring distance is $R=50$. The corresponding angles where the maximum positive errors occur move from $\theta=0$ deg to about 90 deg with increasing L_c/x_0 and Ma. In Fig. 15 the distances R_1 are plotted for $St=0.1$ at which the largest error is ±1 dB. A rough quantitative combined geometric and interference far-field condition may be written for small L_c/x_0 as

$$R_1 \cong 10x_0\exp[2.9\cdot Ma(L_c^2/x_0^2)] \tag{29}$$

In this equation it is assumed that R_1 is proportional to the location x_0 of the peak source intensity. $R>R_1$ is recommended here as a sufficient distance for far-field measurements to become really representative and comparable. It can be seen from Figs. 14 and 15 that special care should be taken with supersonic jets with which a large characteristic source coherence cannot be questioned.

The location x_0 may vary from jet to jet. We suggest that jet noise suppressors tend to reduce this important parameter. x_0 may become longer for hot jets due to the stratification effect of the density gradients. An increased x_0 may also play a role in static-to-flight comparisons when in the latter case there is an outer flow parallel to the jet flow. This situation is studied in more detail in another paper.[14]

For power spectral density measurements the distance x_0 has to be taken for the lowest Strouhal number of interest. Grosche's measurements however were restricted to $St\geq 0.11$. We have therefore assumed $x_0=12$ for $St=0.1$. This value should be sufficient for broadband measurements. Spectra are often measured down to $St=0.02$ or 0.01 where larger values of x_0 are to be expected. If the measurements are made too near to the nozzle, errors have to be expected in the spectra, in the directivities, and in the model laws (Mach number exponents). Since the errors occur at low frequencies the spectra will contain too high or too low intensities at the lower frequency end. The directivities and velocity exponents of jet noise may be measured erroneously due to the angular dependence of the error.

The results of this study should be regarded as preliminary in the sense that more reliable measurements of $L_c(St)$ are required for the whole source region which extends to $x=20$ or 30 for low Strouhal numbers. A comprehensive experimental study of the errors could give further information about the coherence within the source region.

References

[1] Lush, P. A., "Measurements of Subsonic Jet Noise and Comparison with Theory," *Journal of Fluid Mechanics*, Vol. 46, 1971, pp. 477-500.

[2] Ahuja, K. K., "An Experimental Study of Subsonic Jet Noise and Comparison with Theory," *Journal of Sound and Vibration*, Vol. 30, 1973, pp. 317-341.

[3] Tanna, H. K., Dean, P. D., and Fisher, M. J., "The Influence of Temperature on Shock-Free Supersonic Jet Noise," *Journal of Sound and Vibration*, Vol. 39, 1975, pp. 429-460.

[4] Tanna, H. K., "An Experimental Study of Jet Noise, Part I: Turbulent Mixing Noise," *Journal of Sound and Vibration*, Vol. 50, 1977, pp. 405-428.

[5]Tanna, H. K., "An Experimental Study of Jet Noise, Part II: Shock Associated Noise," *Journal of Sound and Vibration*, Vol. 50, 1977, pp. 429-444.

[6]Moore, C. J., "The Role of Shear-Layer Instability Waves in Jet Exhaust Noise," *Journal of Fluid Mechanics*, Vol. 80, 1977, pp. 321-367.

[7]Arndt, R.E.A., Fuchs, H. V., and Michel, U., "Laboratory Study of Jet-Noise Suppressors," *Journal of the Acoustical Society of America*, Vol. 63, 1978, pp. 1060-1068.

[8]Michel, U. and Fuchs, H. V., "The Far Field Condition in Jet Noise Experiments," AIAA Paper 79-0572, 1979.

[9]Maestrello, L., "A Ring-Source Model for Jet Noise," NASA Tech. Memo. 73959, 1978.

[10]Grosche, F. R., "Distribution of Sound Source Intensities in Subsonic and Supersonic Jets," AGARD CP-131, 1974, Paper 4.

[11]Armstrong, R. R., "Einfluss der Machzahl auf die kohärente Turbulenzstruktur eines runden Freistrahls," Dissertation, Technische Universität, Berlin, 1977.

[12]Armstrong, R. R., Michalke, A., and Fuchs, H. V., "Coherent Structures in Jet Turbulence and Noise," *AIAA Journal*, Vol. 15, 1977, pp. 1011-1017.

[13]Michalke, A., "On the Effect of Spatial Source Coherence on the Radiation of Jet Noise," *Journal of Sound and Vibration*, Vol. 55, 1977, pp. 377-394.

[14]Michalke, A., and Michel, U., "Prediction of Jet Noise in Flight from Static Tests," *Journal of Sound and Vibration*, Vol. 67, 1979, pp. 341-367.